



**Ion wave formation during ultracold plasma expansion**E. V. Vikhrov , S. Ya. Bronin, B. B. Zelener, and B. V. Zelener \**Joint Institute for High Temperatures of the Russian Academy of Sciences, Izhorskaya Street 13, Building 2, Moscow 125412, Russia*

(Received 12 May 2021; accepted 25 June 2021; published 19 July 2021)

We present the results of a direct simulation of the expansion of a two-component ultracold plasma for various numbers of particles, densities, and electron temperatures. A description of the expansion process common to all plasma parameters is given. After the escape of fast electrons from the plasma cloud, the excess positive charge is localized at the outer boundary, in a narrow layer. This layer has a characteristic front shape with a sharp drop in the charge concentration. The charged layer retains the remaining electrons during the entire expansion process. As the plasma expands, the speed of movement of the charged layer becomes constant and significantly exceeds the sonic speed of ions. In addition, the dependence of the radial velocity of ions on the radius acquires a self-similar character long before the final stage of expansion. Based on the calculation results, equations and self-similar solutions are obtained. General dependencies on plasma parameters are determined, which are compared with experimental data.

DOI: [10.1103/PhysRevE.104.015212](https://doi.org/10.1103/PhysRevE.104.015212)**I. INTRODUCTION**

The phenomenon of fast acceleration of ions during the free expansion of a dilute plasma is one of the most interesting features of plasma kinetics. The phenomenon was discovered back in 1930 by Tanberg [1] in a pulsed gas discharge. A qualitative explanation of this effect, based on the mechanism of the ambipolar acceleration of ions by electrons, was given only in the early 1960's by Plyutto [2], and also by Hendel and Reboul [3]. The explanation is as follows: Due to the higher mobility of electrons, an electric (ambipolar) field is created, which prevents the escape of electrons and, at the same time, accelerates the ions in the direction of the vacuum or a less dense medium. Later, this phenomenon was observed in the polar wind, cathode flares, vacuum arcs, as well as in exploding wires, laboratory plasma, and in laser sparks. In addition, recent experiments on the creation of jets of high-energy ions from short-pulse interactions with solid targets have revived interest in describing the process of free expansion of plasma into vacuum (see Ref. [4] and references therein). Experimental and theoretical studies (see, for example, the review in Ref. [5] and Refs. [6–9]) carried out in the following years made an additional contribution to the clarification of the ion acceleration process. The description of expanding low-temperature and high-temperature plasmas is possible both based on kinetic equations, hydrodynamic equations, and Maxwell's equations. In this case, rather complex systems of equations are obtained that cannot be solved analytically. Even the numerical solution of these equations for such plasmas causes many problems. Therefore, in order to understand the main processes of plasma expansion, simplified models are mainly used.

New opportunities for studying the expansion of plasma into vacuum have arisen with the creation of an ultracold plasma (UCP). The expansion of the UCP is characterized by well-controlled initial conditions and by relatively slow dynamics, thus creating clear advantages for studying the problem. In addition, the UCP is classical in a wide range of parameters. Moreover, it can be strongly coupled, which makes it possible to study the influence of strong coupling on the expansion of the plasma.

At present, a fairly large amount of experimental material has been obtained on the expansion of the UCP of various elements (Xe, Sr, Rb, Ca) depending on density, the number of particles, and initial temperatures of electrons and ions [10–12]. Many theoretical papers devoted to this problem have been published as well. The review in Ref. [10] notes that there are two alternative approaches to describing the expansion of the UCP. The first approach is associated with the appearance of a local charge imbalance between electrons and ions due to the departure of a part of the fast electrons from the plasma volume. As a result, a space charge arises in the plasma, which forms an electric field. The energy of this field is converted into the kinetic energy of ions, which leads to the expansion of the plasma. An alternative is an approach based on the assumption of electroneutrality and self-similar solutions of the Vlasov equation. This approach is foremost in interpreting the results of the experiment.

All these methods contain various approximations that distort the real picture of the processes that are taking place. One of the best ways to study the UCP expansion process is to simulate it by means of the molecular dynamics (MD) method for a system of interacting  $N_i$  ions and  $N_e$  electrons ( $N_i = N_e = N$ ). However, the implementation of this method for an experimental number of particles  $N = 10^6$ – $10^8$  interacting according to the Coulomb law is a difficult task. So far, calculations have been carried out for the model of a one-component plasma, where the

\*bzelener@mail.ru

ions are considered to be against a uniform background of electrons.

In a previous brief report [13], a few results obtained by means of direct simulation, using the molecular dynamics (MD) method for the expansion of a two-component plasma into a vacuum, were presented. The presented results mainly describe the expansion of a Sr plasma at an initial electron temperature of 100 K. The present paper gives the results of the computation of the expansion of a spherical cloud of a two-component Sr plasma into a vacuum, a wide range of the number of particles, density, and initial temperature of electrons. The density varies from  $10^9$  to  $10^{10}$   $\text{cm}^{-3}$ , the initial electron temperature varies from 25 to 100 K, while the number of particles varies from  $10^3$  to  $10^5$ . It is shown that, at all conditions considered, there is a qualitatively identical character of the expansion process whose individual characteristics take a self-similar form long before the final stage of expansion. It is especially important that the character of the expansion does not change over a wide range of initial electron temperatures. After the escape of fast electrons from the plasma cloud, the excess positive charge is localized at the outer boundary in a narrow layer. This layer has a characteristic front shape with a sharp drop in the charge concentration. As the plasma expands, the speed of movement of the charged layer becomes constant and exceeds the sonic speed of ions significantly. A simple approximate expression for the fraction of electrons leaving the plasma, which depends on a single dimensionless parameter and which is consistent with experiment, has been obtained.

In addition, this paper also presents the results of a calculation of the expansion of a plasma cloud in the form of an oblate ellipsoid of revolution, similar to that realized in experiment [14], but for a smaller number of particles than in the experiment,  $N = 5000$ . A comparison is made with the expansion of a spherical cloud having the same number of particles. It is shown that there is a qualitative agreement between the character of the difference in expansion for these cases with that observed in experiment [14]. It is also shown that the absence of an initial spherical symmetry of the distribution of the charge and the electric field leads to a change in the ratio of the plasma dimensions. For instance, an oblate ellipsoid with a dimension ratio of 1 : 2 turns into an oblong ellipsoid with a size ratio of 1 : 0.84.

## II. PHYSICAL MODEL AND COMPUTATION METHOD

Let us consider a system of particles consisting of singly charged ions and electrons. At the initial moment, the concentrations of electrons and ions in the central point are equal:  $n_{e0} = n_{i0} = n_0$ . In order to avoid computational difficulties, the potential function is modified,

$$U(r_{jk}) = \pm e^2 / (r_{jk} + r_0), \quad (1)$$

where  $j$  and  $k$  are types of particles,  $e$  is the electron charge, and  $r_0$  is a certain minimum distance to which the particles can approach each other. Taking into account the low initial concentrations, this technique is fully justified and does not introduce significant errors. The quantity of  $r_0$  is expressed in

terms of the average distance between particles,

$$r_0 = \alpha(n_0)^{-1/3}, \quad (2)$$

where  $\alpha \sim 0.01$  is small enough not to affect the accuracy of the computations. At zero, the velocities of particles of both types are distributed according to the Maxwell distribution at the given temperature. The initial coordinates are set so that the particle density obeys the normal distribution law, whose dispersion depends on the concentration. In order to integrate the equations of motion, the Verlet scheme in the velocity form is used. The minimum time step for calculating the movement of electrons is  $\tau_e = 10^{-12}$  s. Since the masses of particles differ significantly, the time step is chosen differently for ions and electrons (proportional to the square root of the mass ratio). This technique makes it possible to speed up computations without sacrificing accuracy.

Expansion of a spherical plasma cloud into a vacuum is considered. The initial number of particles  $N$  varies in the computation from  $10^3$  to  $10^5$ . In order to reduce the computation time, a parallelization technique algorithm, specially developed by the authors for their program, is used. Energy conservation is maintained with an accuracy of 1% in the course of the computations. When setting the problem, it is intended to compare the results with the experimental results for Sr [10]. In this connection, the following plasma parameters are chosen: The mass of ions is equal to the mass of the Sr ion; the initial ion temperature  $T_{i0} = 1$  mK,  $T_{e0} = 25$ –100 K, and the initial plasma density is  $n_0 = 10^9$ – $10^{10}$   $\text{cm}^{-3}$ . The main problem posed by the authors is to construct, on the basis of computations made for a different number of particles, general laws for the process of expansion of a plasma cloud depending on the number of particles, and to approach the values of the main characteristics of expansion for maximum numbers  $N \sim 10^8$  corresponding to the experimental data [10]. It turned out that the range of  $N$  from  $10^3$  to  $10^5$  was sufficient for that.

## III. EVAPORATION OF ELECTRONS

The main quantitative characteristic is the total energy  $W$ , which is determined by the excess of the ionizing radiation frequency over the ionization threshold and which is virtually equal to the initial electron energy  $3kT_{e0}N/2$ . The initial spatial distribution of electrons and ions is assumed to be Gaussian,  $n_{i,e}(r) = n_0 \exp(-r^2/2\sigma_0^2)$ ,  $\sigma_0 = (N/n_0)^{1/3}/\sqrt{2\pi}$ . The initial temperature of the ions is  $T_{i0} \sim 1$  mK  $\ll T_{e0}$ . The initial value of the energy of the Coulomb interaction of a random configuration of electrons and ions can be neglected. In contrast to a simple one-component gas, the system under consideration has no simple self-similar relations for the parameters of the system at the later stages of expansion. Nevertheless, numerical calculations make it possible to establish approximate relations for these parameters, namely, the steady-state expansion velocities and the total energy distribution between the electronic and ionic components.

The final distribution of the total energy between the ionic and electronic components depends on the plasma parameters. Plasma expansion begins when the fastest electrons leave it, as a result of which an electric charge  $Q = e\Delta N_e$  is formed in the main plasma region, where  $\Delta N_e$  is the number of electrons that have left the main plasma region. The characteristic time

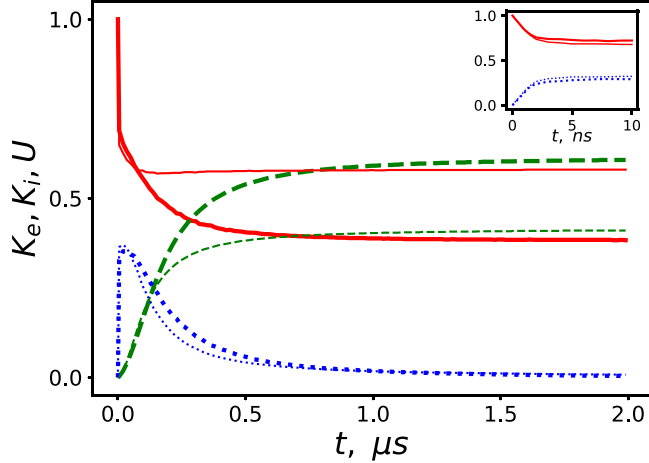


FIG. 1. Kinetic energies of electrons  $K_e$  (red solid lines) and of ions  $K_i$  (green dashed lines) and the energy of the Coulomb interaction  $U$  (blue dotted lines) depending on the expansion time for two values of the initial temperatures:  $T_{e0} = 25$  K (thick lines),  $T_{e0} = 100$  K (thin lines). The inset box reflects the change in the energies at the initial moment.

of this process is of the order of  $t \sim \sigma/v_{Te} = \sigma_0\sqrt{m_e/kT_{e0}} \sim 10^{-7}-10^{-8}$  s. The electrons remaining in the plasma are held in it by means of the potential barrier formed. Pair collisions between electrons and ions scarcely participate in the transfer of energy from electrons to ions. At the beginning of the expansion, the energy of the electrons is converted into the energy of the electric field, which then, by accelerating the ions, transfers the energy to the ionic component. At the final stage of expansion, the energy of the electric field tends to zero and the exchange of energy between the two components of the plasma stops.

Figure 1 shows how the fractions of the three components of the total energy  $W$  change over time for two values of the initial electron temperatures  $T_{e0} = 25$  K (thick lines) and  $T_{e0} = 100$  K (thin lines): the kinetic energy of electrons (red solid lines), the energy of the Coulomb interaction (blue dotted lines), and kinetic energy of ions (green dashed lines) ( $N = 5000$ ,  $n_0 = 3 \times 10^9$  cm $^{-3}$ ). The inset box shows the initial stage of this process.

The kinetic energy of the plasma coincides with an accuracy of several percent with the kinetic energy of ions shown in Fig. 1 by green dashed lines. Accordingly, the kinetic energy of electrons, represented by red solid lines in Fig. 1, is, with an accuracy of several percent, the energy of the electrons that have left the plasma at the beginning of the expansion.

The natural dimensionless parameters on which the expansion parameters can depend are the number of particles  $N$  and the parameter  $N^*$  introduced in Ref. [12],

$$N^* = \frac{3}{2} \sqrt{\frac{\pi}{2}} \frac{kT_{e0}\sigma_0}{e^2}. \quad (3)$$

The characteristic scale of the quantity of the charge is determined by the scale of the energy of the system  $W \sim kT_{e0}N$ ,

$$\frac{Q^2}{\sigma_0} = \frac{e^2 \Delta N_e^2}{\sigma_0} \sim kT_{e0}N \quad (4)$$

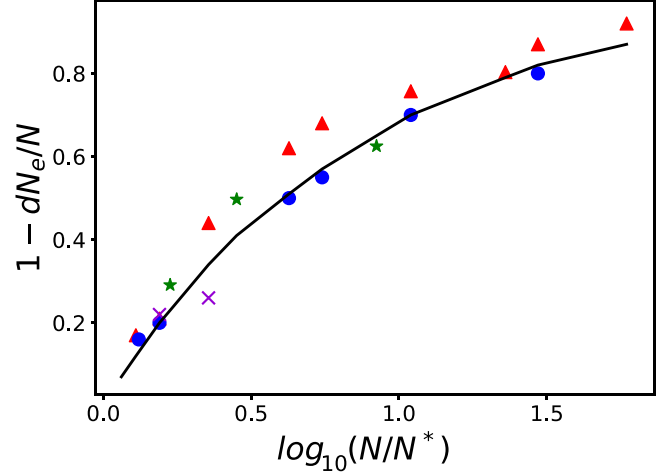


FIG. 2. The fraction of electrons remaining in the plasma is  $1 - \Delta N_e/N$  vs the parameter  $N/N^*$ . The symbols of the experiment [12] are red triangles for  $T_{e0} = 3.9$  K, blue circles for  $T_{e0} = 34.5$  K, violet crosses for  $T_{e0} = 314$  K, and green stars for  $T_{e0} = 813$  K. The solid curve is  $1 - \sqrt{N^*/N}$ .

or

$$\Delta N_e \sim \frac{1}{e} \sqrt{kT_{e0}N\sigma_0} \sim \sqrt{N \cdot N^*}. \quad (5)$$

The experimental results given in Ref. [12] do indicate the presence of a simple approximate relationship between  $\Delta N_e/N$  and  $N^*/N$ . Figure 2 shows the values of the fraction of the electrons remaining in the plasma  $1 - \Delta N_e/N$  (symbols) obtained in the experiment [12], depending on the parameter  $N/N^*$  for different initial temperatures of electrons. Red triangles indicate the results corresponding to  $T_{e0} = 3.9$  K, blue circles mean  $T_{e0} = 34.5$  K, violet crosses mean  $T_{e0} = 314$  K, and green stars mean  $T_{e0} = 813$  K. The solid curve represents the approximate expression for the value under consideration,  $1 - \Delta N_e/N \approx 1 - \sqrt{N^*/N}$ , following from (5).

#### IV. ION FRONT FORMATION

The excess positive charge remaining in the plasma is localized in a narrow layer at the outer boundary of the plasma for  $r > 2\sigma(t)$  [ $\sigma^2(t) = \langle r^2 \rangle / 3$ ]. Averaging in the definition of  $\sigma(t)$  is performed with the ionic distribution function. The characteristic time of its formation is determined by the ion velocity and the plasma size  $t \sim \sigma_0/\sqrt{kT_{e0}/m_i}$ . Under typical experimental conditions and the computation parameters presented here, this value is of the order of a microsecond. According to numerical computations, this layer has a characteristic front shape, with a sharp drop in the charge concentration. Figure 3 shows the radial distribution functions of ions  $f_i$  and electrons  $f_e$  and the Gaussian distribution depending on  $\xi = r/\sigma(t)$  for  $N = 5000$ ,  $T_{e0} = 50$  K, and  $n_0 = 3 \times 10^9$  cm $^{-3}$  at different times. As shown in Ref. [13], one-dimensional distributions that are determined in experiments are virtually not distorted. Distortion of the radial distribution becomes less noticeable at the final stage of expansion. As the plasma expands, the velocity of movement of the charged layer  $V_Q$ , as well as  $V_\sigma = d\sigma(t)/dt$ , become constant while maintaining the ratio between them at the level of 2.5.

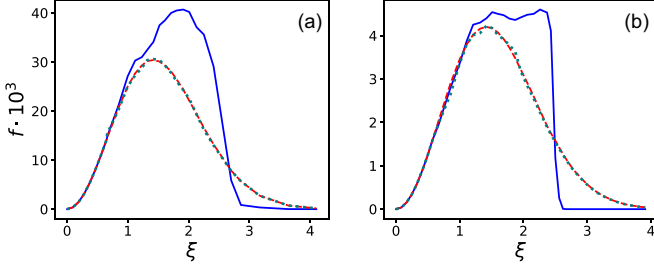


FIG. 3. Distribution functions of ions  $f_i$  (blue solid line) and electrons  $f_e$  (green solid line) and the Gaussian distribution  $\sim \xi^2 \exp(-\xi^2/2)$  (red dotted line) depending on  $\xi = r/\sigma(t)$ . (a)  $t = 1 \mu\text{s}$ , (b)  $t = 10 \mu\text{s}$ .

The radial dependence of the electric field has a pronounced maximum in the region of the charged layer. Let us define the dimensionless strength  $\mathcal{E}$  of the electric field  $E(r, t)$  by the equality

$$E(r, t) \approx \frac{e\Delta N_e}{\sigma^2(t)} \mathcal{E}(\xi), \quad \xi = r/\sigma(t). \quad (6)$$

The dimensionless function  $\mathcal{E}(\xi)$  of the dimensionless quantity  $\xi$  is approximately the same for all values of the plasma parameters at the times when the layer of positive charge has had time to form. In a wide range of plasma parameters at this stage of plasma expansion, the function  $\mathcal{E}(\xi)$  is practically the same and has a characteristic maximum near the value of  $\xi \approx 2.5$ . Figure 4 shows the values of  $\mathcal{E}(\xi)$  depending on the number of particles, density, temperature, and expansion time.

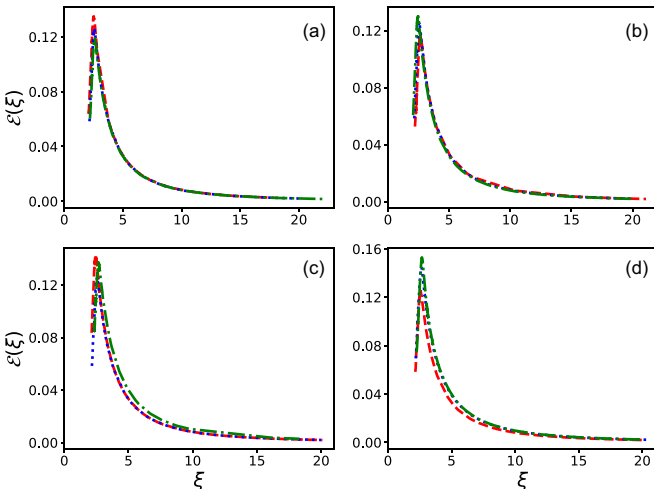


FIG. 4. Dimensionless function  $\mathcal{E}(\xi)$  (6). (a)  $\mathcal{E}(\xi)$  for  $N = 5000$ ,  $T_{e0} = 50 \text{ K}$ ,  $n_0 = 3 \times 10^9 \text{ cm}^{-3}$ , and three values of time:  $t = 10, 15$ , and  $20 \mu\text{s}$ . (b)  $\mathcal{E}(\xi)$  for  $N = 5000$ ,  $n_0 = 3 \times 10^9 \text{ cm}^{-3}$ ,  $t = 15 \mu\text{s}$ , and three values of the electron temperature:  $T_{e0} = 25, 50$ , and  $100 \text{ K}$ . (c)  $\mathcal{E}(\xi)$  for  $N = 5000$ ,  $t = 15 \mu\text{s}$ ,  $T_{e0} = 50 \text{ K}$ , and three values of density:  $n_0 = 10^9, 3 \times 10^9$ , and  $10^{10} \text{ cm}^{-3}$ . (d)  $\mathcal{E}(\xi)$  for  $t = 15 \mu\text{s}$ ,  $T_{e0} = 50 \text{ K}$ ,  $n_0 = 3 \times 10^9 \text{ cm}^{-3}$ , and three values of  $N = 5000, 12\,500$ , and  $25\,000$ .

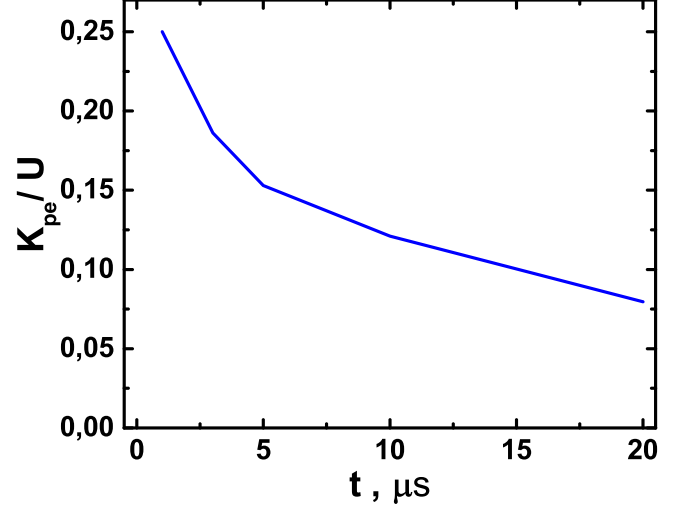


FIG. 5. The dependence  $K_{pe}/U$  on the time.

## V. IONIC WAVE

### A. Spherical symmetry of the initial conditions

At the final stage of expansion, the amplitude of the electric field decreases  $\sim 1/t^2$ , however, the weakening field is sufficient to confine the remaining electrons in the plasma region during the entire expansion process. These electrons account for no more than 5% of the kinetic energy in this region, which is determined by the kinetic energy of the ions. The kinetic energy of these electrons decreases faster than the height of the barrier holding them in the plasma.

Figure 5 shows the ratio of the average energy of plasma electrons  $K_{pe}$  to the height of the barrier holding them  $U$  for  $N = 5000$ ,  $T_{e0} = 100 \text{ K}$ , and  $n_0 = 3 \times 10^9 \text{ cm}^{-3}$ ,

$$U = e \int_0^\infty E(r) dr = \frac{e^2 \Delta N_e}{\sigma(t)} \int_0^\infty \mathcal{E}(\xi) d\xi \approx \frac{e^2 \Delta N_e}{3\sigma(t)}. \quad (7)$$

The thermal energy of ions is always negligible in comparison with the energy of their radial motion. The dependence of the radial velocity of ions on the radius acquires a self-similar character  $V_{ir}(r, t) = r/t$  long before the final stage of expansion, immediately after the formation of the charged layer. Figure 6 shows the dependences of  $tV_{ir}(r, t)/r$  on  $\xi = r/[\sigma(t)]$  for the plasma parameters corresponding to Fig. 1 ( $T_{e0} = 100 \text{ K}$ ) and for three times,  $t = 15 \mu\text{s}$  (blue solid line),  $t = 2 \mu\text{s}$  (red dotted line), and  $t = 1 \mu\text{s}$  (green dashed line). The figure shows that the steady-state self-similar distribution  $V_{ir}(r, t)$  is slightly, within 5%, violated in the region of the positively charged layer  $\xi > 2$ . Neglecting the thermal energy of the ions, their kinetic energy is equal to

$$\begin{aligned} K_i &= \frac{m_i}{2} \int n_i(r, t) V_{ir}^2(r, t) dr \\ &= \frac{m_i}{2} N \langle r^2 \rangle / t^2 = \frac{3m_i}{2} N \sigma^2(t) / t^2. \end{aligned} \quad (8)$$

It follows from this that the plasma expansion velocity  $V_\sigma = d\sigma(t)/dt$  becomes constant  $V_\sigma = \sqrt{2K_i/3m_iN}$  at the final stage of expansion, when the electric energy can be neglected, and when the kinetic energies of the plasma components stop

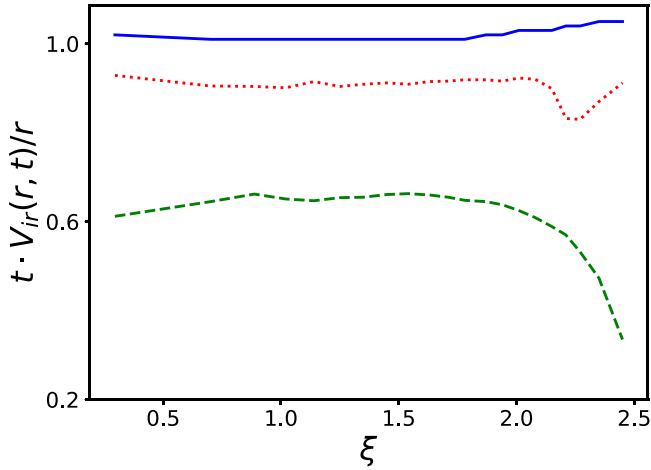


FIG. 6. The dependencies of  $tV_{ir}(r, t)/r$  on  $\xi = r/[\sigma(t)]$  for plasma parameters corresponding to Fig. 1 ( $T_{e0} = 100$  K) for three values of time:  $t = 15 \mu\text{s}$  (blue solid line),  $t = 2 \mu\text{s}$  (red dotted line), and  $t = 1 \mu\text{s}$  (green dashed line).

changing. Note that the last equality does not imply a Gaussian distribution of the ion concentration.

Numerical calculations by the MD method show that the ratio of the kinetic energy of ions  $K_i$  to the total energy of the system  $W \approx 3k_b T_{e0} N/2$  at large values of  $N$ , typical for the conditions of most experiments, tends to 1. This ratio *per se* is, with good accuracy, a function of the value of the dimensionless parameter  $N/N^*$  introduced in Ref. [12]. Figure 7 shows the dependence of the ratio of  $K_i/W$  on  $N/N^*$  for three density values,  $n_0 = 10^9 \text{ cm}^{-3}$  (green pentagons),  $n_0 = 3 \times 10^9 \text{ cm}^{-3}$  (blue crosses), and  $n_0 = 10^{10} \text{ cm}^{-3}$  (red stars), and for three values of temperature,  $T_{e0} = 25, 50$ , and

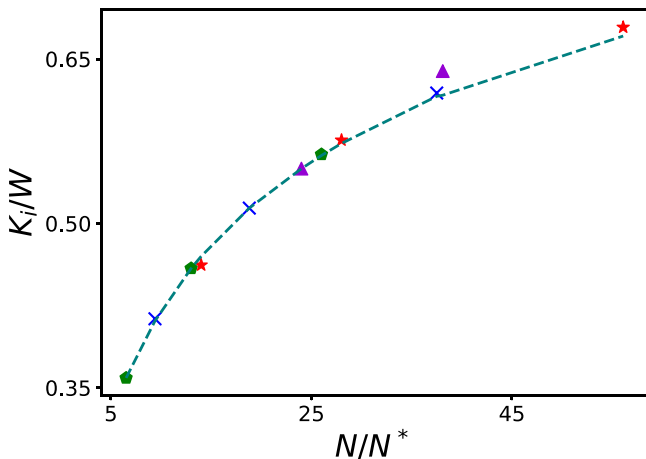


FIG. 7. The fraction of the kinetic energy of ions  $K_i/W$  depending on  $N/N^*$ : (1)  $n_0 = 10^9 \text{ cm}^{-3}$ ,  $N = 5000$ , and for three temperature values:  $T_{e0} = 25, 50$ , and  $100$  K (green pentagons, the values of  $K_i/W$  decrease with increasing  $T_{e0}$ ). (2)  $n_0 = 3 \times 10^9 \text{ cm}^{-3}$ ,  $N = 5000$ ,  $T_{e0} = 25, 50$ , and  $100$  K (blue crosses). (3)  $n_0 = 10^{10} \text{ cm}^{-3}$ ,  $N = 5000$ ,  $T_{e0} = 25, 50$ , and  $100$  K (red stars). (4)  $n_0 = 3 \times 10^9 \text{ cm}^{-3}$ ,  $N = 5000$ ,  $T_{e0} = 50$  K, and  $N = 12500$  and  $50000$  (purple triangles, the values of  $K_i/W$  grow with  $N$  growing). (5) The teal dashed line is the fit.

100 K for each, and for three values of  $N = 5000, 12500$ , and  $50000$  (purple triangles) at  $T_{e0} = 50$  K. For large values of  $N$ , the ratio of  $K_i/W$  is close to 1, and the expansion rate tends to the value  $V_\sigma = \sqrt{k_b T_{e0}/m_i}$ , which is consistent with the experimental data presented in Ref. [12]. The speed of movement of the charged layer  $V_Q$ , which can be compared with the speed of movement of the maximum of the field strength, also becomes constant at the final stage of expansion and is determined by the following relation:

$$V_Q \approx 2.5V_\sigma. \quad (9)$$

### B. Cylindrical symmetry of the initial conditions

The above calculations showed that all stages of the plasma cloud expansion were affected by the electric field of the charged ion layer formed at the initial stage. The formation of the charged layer of ions and the electric field depends on the initial distribution function. In the case of the spherical symmetry of the initial conditions, the charged layer has spherical symmetry which is conserved over time. However, in the case of the cylindrical symmetry of the initial functions, the charged layer has the same symmetry. Specific features of this distribution are sustained over time, up to the final stage of expansion.

In Ref. [14], experimental results on the expansion of a plasma with a cylindrical initial configuration are presented,

$$n_{i,e}(x, \rho) = n_0 \exp(-\sqrt{x^2 + \rho^2}/4/\sigma), \quad (10)$$

where  $\rho^2 = y^2 + z^2$ ,  $\sigma^3 = N/32\pi n_0$ . The paper compares the expansion dynamics for a spherically symmetric Gaussian initial distribution and a cylindrical distribution (10). Along with the above-described computations of the spherically symmetric expansion by the MD method, the authors have performed similar computations for the initial density distribution (10). The computations are performed for the number of particles  $N = 5000$ , which is less than that in the experiment, and because of this, the length scales and timescales differ from the experimental conditions. The density and temperature of the electrons are chosen in the calculations so that the expansion velocities, depending on  $T_{e0}$  and  $N/N^*$ , are close to the experimental values. Figure 8 shows the calculated values of the  $v_x$  component for two versions of the initial distribution: Gaussian distribution,  $n_0 = 3 \times 10^9 \text{ cm}^{-3}$ , exponential distribution (10),  $n_0 = 10^{10} \text{ cm}^{-3}$ , and for four times: (a)  $t = 0.2 \mu\text{s}$ , (b)  $t = 0.5 \mu\text{s}$ , (c)  $t = 1 \mu\text{s}$ , and (d)  $t = 3 \mu\text{s}$ . The initial value of the electron temperature is  $T_{e0} = 100$  K. The computation results presented qualitatively reproduce the experimental results presented in Ref. [14]. The absence of spherical symmetry in the initial configuration gives rise to a nonuniform distribution of the emerging field. This is due to the fact that at the initial stage of expansion, it is easier for electrons to leave the plasma in the direction of the  $x$  axis, since the dimension of the plasma in this direction is half as large and, accordingly, lower decelerating resistance of ions takes place.

Heterogeneity of the charge and electric field distribution is clearly manifested in the change in the ratio of the plasma dimensions. At the initial time,  $\langle x^2 \rangle = 4\sigma^2$  and  $\langle \rho^2 \rangle = 32\sigma^2$ , so that the initial ratio of diameter to height is

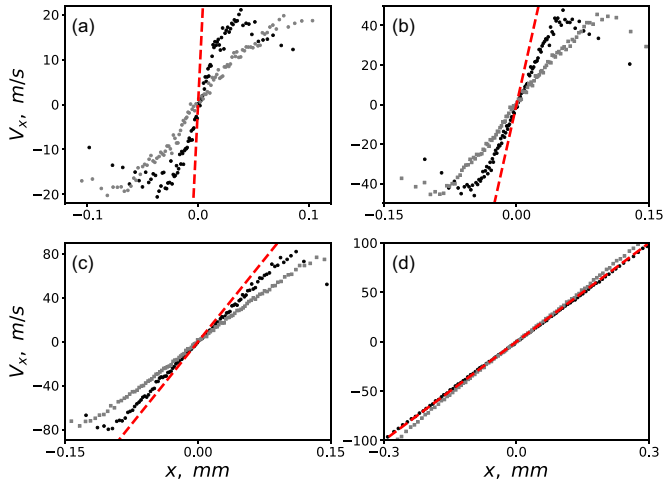


FIG. 8. Calculated values of the  $v_x$  component for two versions of the initial distribution: Gaussian distribution (gray circles),  $n_0 = 3 \times 10^9 \text{ cm}^{-3}$ , and exponential distribution (black circles),  $n_0 = 10^{10} \text{ cm}^{-3}$ , for four times: (a)  $t = 0.2 \mu\text{s}$ , (b)  $t = 0.5 \mu\text{s}$ , (c)  $t = 1 \mu\text{s}$ , (d)  $t = 3 \mu\text{s}$ . The initial value of the electron temperature is  $T_{e0} = 100 \text{ K}$ . The red dashed line is for  $x/t$ .

$k = \sqrt{\langle \rho^2 \rangle / 2 \langle x^2 \rangle} = 2$ . Due to the nonuniformity of the field, the characteristic size of the plasma in the  $x$  direction grows faster than its transverse size and, as a result of that, the ratio of these sizes changes to the opposite. Figure 9 shows the time dependence of the value  $k = \sqrt{\langle \rho^2 \rangle / 2 \langle x^2 \rangle}$  for the next values of the plasma parameters:  $T_{e0} = 100 \text{ K}$ ,  $n_0 = 10^{10} \text{ cm}^{-3}$ ,  $N = 5000$ . It can be seen from Fig. 9 that the size ratio decreasing with time does not stop at 1, which would correspond to spherical symmetry, but continues to decrease to a value of 0.84.

A similar ratio of dimensions takes place for a charged layer as well. Figure 10 shows the values of the electric field intensity along the axis of symmetry  $E(x, 0)$  (blue solid curve) and in the transverse direction  $E(0, \rho)$  (red dashed curve). The plasma parameters are the same as in Fig. 8 at  $t = 30 \mu\text{s}$ .

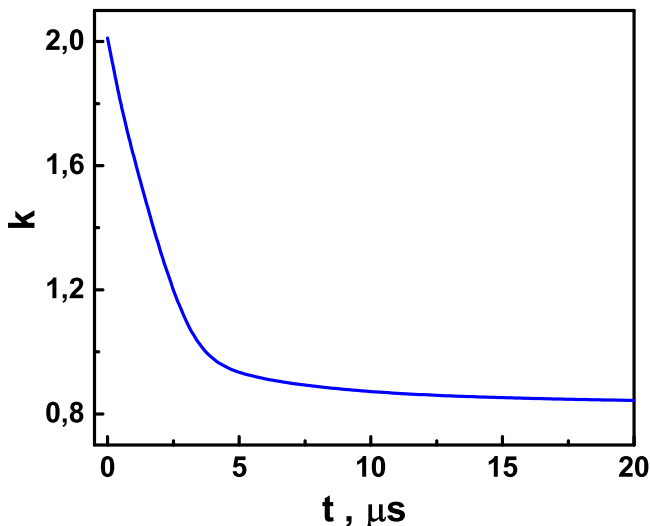


FIG. 9. Time dependence of the ratio of diameter to height  $k = \sqrt{\langle \rho^2 \rangle / 2 \langle x^2 \rangle}$ .

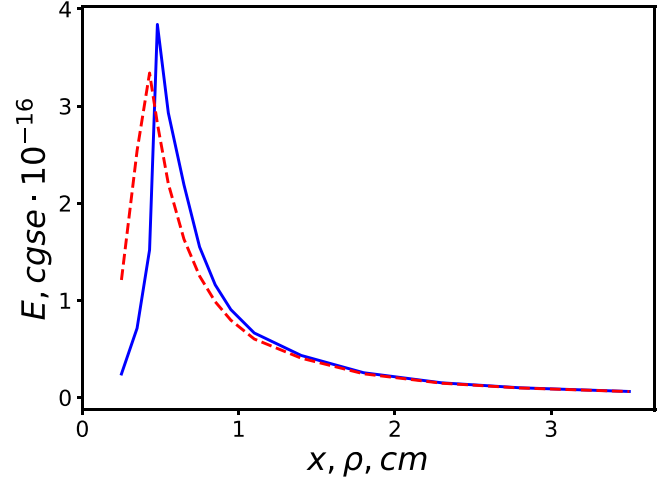


FIG. 10. Electric field intensity in CGSE units along the axis  $E(x, 0)$  (blue solid curve) and in the transverse direction  $E(0, \rho)$  (red dashed curve) at  $t = 30 \mu\text{s}$ ,  $n_0 = 10^{10} \text{ cm}^{-3}$ ,  $T_{e0} = 100 \text{ K}$ .

## VI. CONCLUSION

This paper presents detailed results of the simulation of the expansion of a spherical cloud of a two-component Sr plasma into vacuum. The dependence of all characteristics of expansion on the number of particles, density, and initial temperatures of electrons is determined, and equations for the distribution functions are formulated. Self-similar solutions are obtained for various stages of expansion. It is shown that under all the conditions considered, the same character of the expansion process takes place. At the initial stage, after the escape of fast electrons from the plasma cloud, the excess positive charge is localized at the outer boundary, in the form of a narrow front of ions with a sharp decrease in the charge concentration. As the plasma expands, the front velocity becomes constant and significantly exceeds the sound velocity of the ions. In addition, the dependence of its velocity on the radius has a self-similar character long before the final stage of expansion. A comparison of various experimental data with simulation results is carried out.

In addition, this work also gives the results of calculating the expansion of a cylindrical plasma cloud for the number of particles  $N = 5000$ ,  $n_0 = 10^{10} \text{ cm}^{-3}$ ,  $T_{e0} = 100 \text{ K}$ . It is shown that there is a qualitative agreement between the character of the difference in expansion for spherical and cylindrical symmetry with what is observed in the experiment [14]. In this case, the absence of spherical symmetry of the charge and electric field distribution is clearly manifested in the change in the ratio of the plasma dimensions.

## ACKNOWLEDGMENTS

The calculations were performed at the Joint Supercomputer Center of RAS and at the Supercomputer Center of Keldysh Institute of Applied Mathematics of RAS. The work was supported by the Russian Science Foundation Grant No. 18-12-00424. The work on the theoretical analysis of a cylindrical symmetry was supported by the Ministry of Science and Higher Education of the Russian Federation (State Assignment No. 075-00460-21-00).

- [1] R. Tanberg, *Phys. Rev.* **35**, 1080 (1930).
- [2] A. A. Plyutto, *Zh. Eksp. Teor. Fiz.* **39**, 1589 (1960).
- [3] H. W. Hendel and T. T. Reboul, *Phys. Fluids* **5**, 360 (1962).
- [4] P. Mora, *Phys. Rev. E* **91**, 013107 (2015).
- [5] C. Sack and H. Schamel, *Phys. Rep.* **156**, 311 (1987).
- [6] P. Mora, *Phys. Plasmas* **12**, 112102 (2005).
- [7] D. Bennaceur-Doumaz, D. Bara, E. Benkhelifa, and M. Djebli, *J. Appl. Phys.* **117**, 043303 (2015).
- [8] I. S. Elkamash and I. Kourakis, *Phys. Rev. E* **94**, 053202 (2016).
- [9] Y. Hu and J. Wang, *Phys. Rev. E* **98**, 023204 (2018).
- [10] T. C. Killian, T. Pattard, T. Pohl, and J. M. Rost, *Phys. Rep.* **449**, 77 (2007).
- [11] M. Lyon and S. L. Rolston, *Rep. Prog. Phys.* **80**, 017001 (2017).
- [12] T. C. Killian, S. Kulin, S. D. Bergeson, L. A. Orozco, C. Orzel, and S. L. Rolston, *Phys. Rev. Lett.* **83**, 4776 (1999).
- [13] E. V. Vikhrov, S. Ya. Bronin, A. B. Klayrfeld, B. B. Zelener, and B. V. Zelener, *Phys. Plasmas* **27**, 120702 (2020).
- [14] M. K. Warrens, G. M. Gorman, S. J. Bradshaw, and T. C. Killian, *Phys. Plasmas* **28**, 022110 (2021).